Available online at www.sciencedirect.com
SCIENCE DIRECT
Composites: Part B 37 (2006) 418–424
composites Part B: engineering
www.elsevier.com/locate/compositesb

Development of CNT/Si_3N_4 composites with improved mechanical and electrical properties

Csaba Balázsi [a,*], Balázs Fényi [b], Norbert Hegman [b], Zsuzsanna Kövér [a], Ferenc Wéber [a], Zofia Vértesy [c], Zoltán Kónya [d], Imre Kiricsi [d], László Péter Biró [c], Péter Arató [a]

[a] *Ceramics and Composites Laboratory, Research Institute for Technical Physics and Materials Science, Hungarian Academy of Science, P.O. Box 49, Budapest XII, Konkoly-Thege út 29-33, H-1121 Budapest, Hungary*
[b] *Department of Ceramics and Silicates Engineering, University of Miskolc, H-3515 Miskolc Egyetemváros, Hungary*
[c] *Nanotechnology Department, Research Institute for Technical Physics and Materials Science, Konkoly-Thege út 29-33, H-1121 Budapest, Hungary*
[d] *Department of Applied and Environmental Chemistry, University of Szeged, Rerrich Béla tér 1., H-6720 Szeged, Hungary*

Received 7 April 2005; received in revised form 18 July 2005; accepted 25 July 2005
Available online 29 March 2006

Abstract

Silicon nitride based composites with different amount (1, 3 or 5 wt%) of carbon nanotubes have been prepared by using hot isostatic pressing. Composites with 1, 5 or 10 wt% carbon black and graphite have been manufactured, in comparison. Optimisation of the manufacturing processes has been performed, providing intact carbon nanotubes during high temperature sintering. In the case of 1 or 3 wt% carbon nanotube addition, the increase of gas pressure during sintering resulted in an increase of bending strength. It was found that microstructure features achieved by properly designed sintering parameters are the main responsible factors for the strength improvements. Scanning electron microscopy showed that carbon nanotubes have a good contact to the surface of silicon nitride grains. The electrical properties of silicon nitride matrices with carbon addition may change essentially.

Keywords: A. Ceramic-matrix composites (CMCs); Carbon nanotubes; Silicon nitride; B. Mechanical properties; B. Electrical properties

1. Introduction

As resulted from several theoretical calculations, carbon nanotubes (CNTs) are characterised by exceptional mechanical and electrical properties [1–5]. Therefore, it is expected that the addition of CNTs will radically improve the quality of different matrices, such as polymer, metal and ceramic. Till now, only modest improvements of properties were reported in CNTs reinforced silicon carbide [6] and silicon nitride matrix composites [7], whereas a noticeable increase of the fracture toughness and of electrical conductivity has been achieved in CNTs reinforced alumina matrix composites [8,9]. Another research group have found rather low increments in toughness, but significantly improved the contact damage for these composites [10,11]. The CNTs placed to the grain boundaries in alumina which can provide shear weakness under indentation could explain this phenomenon. In order to get the full use of the benefits provided by CNTs it is crucial to achieve a good dispersion of CNTs in the ceramic matrix. Retaining the CNTs un-attacked in the composites and to optimise the interfacial bonding between CNTs and matrix are the further requirements. In this way, the toughening effects characteristic to micron-scale fibre composites could be explored: crack bridging by CNTs, CNT pullout on the fracture surfaces and crack deflection at the CNT/matrix interface [12].

In this work, we focused on preparation processes to tailor the microstructure of carbon nanotube reinforced silicon nitride-based ceramic composites. Development of the processes has been conducted to effectively disperse the CNTs in the matrix. An optimisation of temperature–pressure-holding time relation was performed to preserve the carbon nanotubes in composites and to avoid damaging during high temperature processing.

Secondly, the effect of different carbon additions on the impedance spectrum of composites was investigated with a phase sensitive 'lock-in' measuring system. Alternative current (AC) impedance spectroscopy provides knowledge on different contribution of grain bulk, grain boundary, contacts and other additives of granular composite materials.

* Corresponding author. Tel.: +36 1 392 2222/3279; fax: +36 1 392 2226.
E-mail address: balazsi@mfa.kfki.hu (C. Balázsi).

1359-8368/$ - see front matter © 2006 Elsevier Ltd. All rights reserved.
doi:10.1016/j.compositesb.2006.02.006

As answer to voltage bias of the signal generator current signal was detected separated in two components as in-phase and quadrature (respect to excitation voltage phase), from which the complex impedance was calculated up to 100 kHz in our investigation. To verify the suitability of the impedance measurements a well-known ceramic ionic conductor was simulated by a series of two parallel RC circuits, taking its parameters from the literature. Previously, four point resistance measurements were carried out to calculate the DC conductivity of different carbon added samples without the influence of undesired contact resistance. In the following sections, morphological, structural observations, as well as characterisation of mechanical and electrical properties will be presented.

2. Experimental details

Details about composition of the starting powder mixtures and preparation can be seen in Table 1. Si_3N_4 (Ube, SN-ESP), AlN (H.C. Starck, grade C), Al_2O_3 (Alcoa, A16) and Y_2O_3 (H.C. Starck, grade C) were used as starting powders. To vary the sintering conditions, AlN was introduced to some of the batches. Different amount of CNTs (multiwall carbon nanotubes, produced as described elsewhere [13]) were added in addition to batches (1, 3, 5 wt%). Furthermore, in comparison carbon black (Taurus Carbon Black, N330, average particle size between ~50 and 100 nm) and graphite (Aldrich, synthetic, average particle size 1–2 μm) were also added to batches. The powder mixtures together with the carbon additions were milled in ethanol in a planetary type alumina ball mill for 3 h. In some cases, the powder mixtures and CNTs were introduced in an ethanol bath and intensively sonicated together. After sonication surfactants (polyethylen-glycol, PEG) were added to the powder mixture. The batches were dried and sieved. Green samples were obtained by dry pressing at 220 MPa.

Hot isostatic pressing (HIP) was performed at 1700 °C in high purity nitrogen by a two-step sinter-HIP method using BN embedding powder. The heating rate was not exceeding 25 °C/min. The gas pressure and holding time were also varied. The dimensions of the as-sintered specimens were 3.5×5×50 mm. After sintering, the weight change of the samples was determined. All surfaces of the samples were finely ground on a diamond wheel, and the edges were chamfered. The density of the sintered materials was measured by Archimedes method. Phase compositions were determined by Philips PW 1050 diffractometer. Morphology of the solid products was studied by field emission scanning electron microscope, LEO 1540 XB. For HIP samples the elastic modulus and the three-point bending strength were determined by a bending test with spans of 40 and 20 mm.

2.1. Preparation of contacts for electrical measurements

To contact the ceramics samples first, the contact places (four for every sample) were masked out and a thin gold layer was evaporated on it in a vacuum chamber. Then silver grains containing composite glue was applied and dried. This surface could be soldered producing bounding to the electrical wires of electric measurements.

2.2. AC measurements

In our work, a phase sensitive 'lock-in' complex impedance measurements were carried out. First, to verify the measuring arrangement a defined model electronic circuit was measured, which simulated an ionic conductor sample taken from literature [14]. The circuit contained two serial connected parallel R_1–C_1 and R_2–C_2 elements with different resonance frequencies. The analytical fit of double R–C elements agreed well with the measuring points in the 100 Hz–100 kHz frequency range we applied.

The measurement set up can be seen in Fig. 1, where the sample was substituted by electronic circuit (in the insert) in the case of calibration. The signal generator output was

Table 1
Starting compositions and preparation conditions of sintered samples

Batch	Starting powders (wt%)				CNT (MWNT) (wt%)	CB (carbon black) (wt%)	Gr (graphite) (wt%)	Ball milling (in ethanol, h)	Ultrasonic agitation (in ethanol)	Sintering conditions		
	Si_3N_4	AlN	Al_2O_3	Y_2O_3						Temperature (°C)	Holding time	Pressure (MPa)
672	90	0	4	6	–			3	–	1700	–	2
728	90	0	4	6	–	10		3	–	1700	–	2
729	90	0	4	6		1		3		1700	–	2
730	90	0	4	6	–		10	3	–	1700	–	2
731	90	0	4	6	–		1	3		1700	–	2
734	90	0	4	6	1			3	–	1700	–/3 h	2/20
735	87	4	4	5	1			3	–	1700	–	2
736	90	0	4	6	5			3	–	1700	–	2
750	87	4	4	5	5			3	1 h (mixture+MWNT)	1700	–	2
751	90	0	4	6	–	5		3	–	1700	–	2
752	90	0	4	6	–		5	3		1700	–	2
766	90	0	4	6	3			3	3 h (mixture+MWNT)	1700	3 h	20

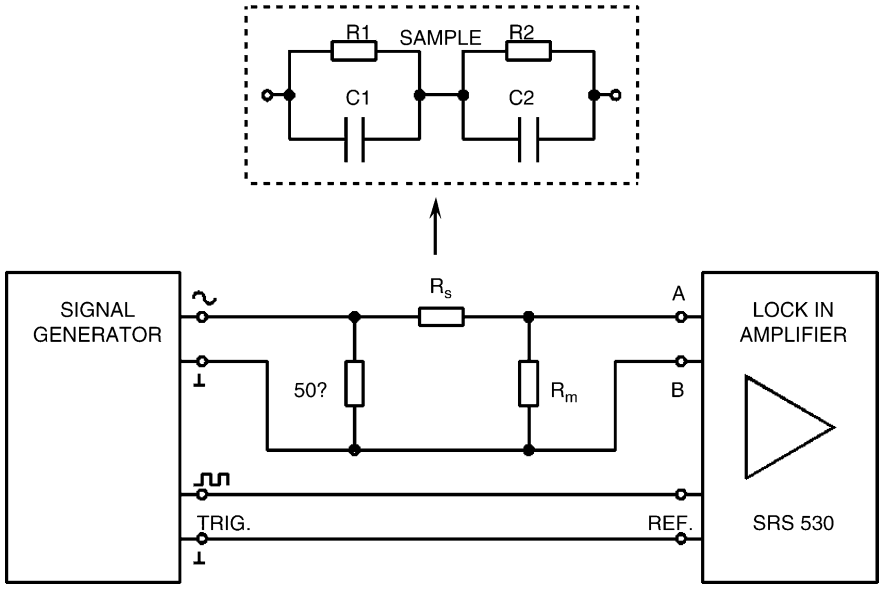

Fig. 1. Measurement setup of AC impedance measurements, and electronics circuit as a model sample for verifying the method.

terminated by 50 Ω due to the generator calibration to this termination. Then a generator voltage output was connected to a serial R_s and R_m resistance ($R_s \gg R_m$). R_s is the measurable sample changing its value in a wide range and R_m is about two order less reference resistance value to measure the current in the circuit, without influence the voltage drop on R_s sample. The voltage drop on the known ohmic resistance R_m was connected to the lock-in detector (SRS 530) to measure the current in the circuit. The reference signal input for the lock-in amplifier orthogonal system was taken by the signal generator trigger channel with the same phase as the signal channel had. Therefore, the current amplitude and phase of the measurable sample were detected respect to voltage drop vector on the measurable sample. The later was easily calculated by the generator voltage setup and small correction by R_m. After measuring the two components of the current through, the sample impedance was evaluated according to Ohm's law.

2.3. DC measurements

DC conductivity determination was carried out by four point contact measurements using a high impedance multimeter (Agilent34970A) up to 10 MΩ overall termination. Samples with higher impedance showed overload in DC measurements, their impedance however could be measured by AC method increasing the excitation frequency.

3. Results and discussions

Morphological observations of fracture surfaces of HIP processed samples are presented in Fig. 2. As it is shown in Fig. 2, after sintering the CNTs are preserved in the structure. Some degradation of nanotubes may occur during sintering [7,16], but it was not observed in this case. The CNTs are located mainly in the inter-granular places and they are well attached to the silicon nitride grains. In the same time adhered carbon nanotubes to each other can be observed (Fig. 2a and b). The proper separation and dispersion of carbon nanotubes proved to be a difficult task of composite preparation. The ball milling was followed by ultrasonic agitation of MWNT-powder mixtures for gaining a better homogeneity. By increasing the sonication time little advances have been achieved, but the tendency of nanotubes, the strong adherence and linking behavior to each other could not be totally suppressed. As can be observed, the CNTs in most of the cases are in groups, they can be found as nano- or micrometer sized islands in the matrix after sintering (Fig. 2a and b). By increasing the pressure from 2 to 20 MPa and holding time to 3 h a totally different microstructure have been developed. A grain growing process accompanied by a phase transformation can be observed in the microstructure of the 1 and 3 wt% CNT containing sample (73410 and 76605, Fig. 2c. and d). Huge β-Si_3N_4 grains (several micro meters in length) developed during the sintering process. As can be seen in Fig. 2c (73400), a homogeneous distribution of CNTs can be achieved with good contact to grain surface in certain places. For this reason, CNT added samples had larger porosity than reference samples (batch 672) and the reinforcement processes (e.g. pullouts, crack bridging, crack deflection) are still not enough for a significant global strengthening (Figs. 4 and 5).

A phase transformation from α-Si_3N_4 to β-Si_3N_4 is taking place in the case of reference sample (67236, Fig. 3a). The same transformation was observed in the case of all of the composites as well. The main constituents of composites were α-Si_3N_4, JCPDS-PDF 41–360 and β-Si_3N_4, JCPDS-PDF 33-160 (as in Fig. 3). In the case of 73400 (1% CNT) prepared at higher pressure and longer sintering time all of the structure is transforming to β-Si_3N_4.

A linear relation between apparent density and modulus of composites is presented in Fig. 4. The reference sample without

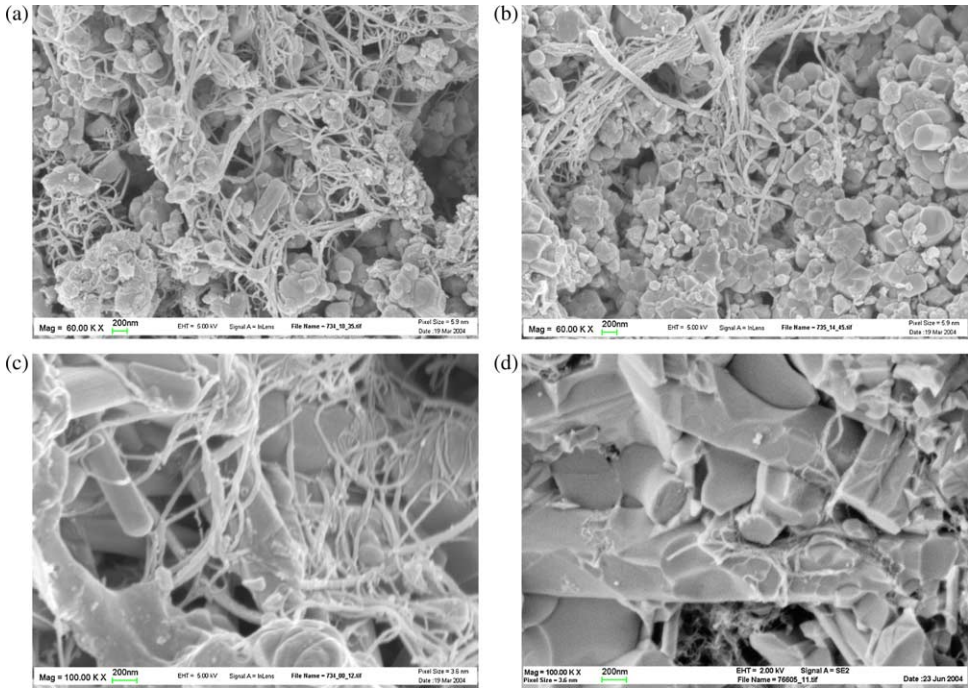

Fig. 2. Fracture surfaces of CNT/Si_3N_4 composites with different compositions prepared at 1700 °C, 2 MPa, without holding time (a) 73410 (1% CNT), (b) 73515 (1% CNT) and CNT/Si_3N_4 composites prepared at higher pressures (20 MPa) and longer sintering times (3 h) at 1700 °C (c) 73400 (1% CNT) and (d) 76605 (3% CNT).

any nanotube addition has the highest degree of densification connected to highest modulus value. As can be observed in the case of composites prepared at lower pressure (2 MPa), with CNT addition the porosity has been increased which had a detrimental role to modulus. By increasing the gas pressure (and holding time) the same level of densification can be achieved for composites with 1% CNT (batch 734) as for reference sample realised at low pressures (batch 672). In the case of 1% CNT addition, a higher densification level, but similar modulus values could be realised with increasing the pressure from 2 to 20 MPa. As a general rule, at high pressures (20 MPa), with increasing the CNT content a decrease of modulus can be observed, similar to the observations made at low pressures (2 MPa).

The relationship between apparent density and three point bending strength of composites and reference sample can be seen on Fig. 5. The general tendency is similar to the modulus namely, the decrease of strength with increasing the CNT content is maintained at low pressures (2 MPa), as well as at high pressures (20 MPa). In this case however, the effect of pressure and holding time is more striking. Comparing the composites with the same CNT content, higher strengths were achieved by increasing the sintering pressure (and holding time) to 20 MPa. In the case of samples with 1% CNT content (batch 734), applying a higher sintering pressure a higher compaction level and an increase by 100%, from an average strength level of 300–600 MPa, can be achieved. This sample was found to have the highest degree of densification connected to highest strength (even higher than for reference sample without any nanotube addition prepared at low pressure).

As resulted from Figs. 4 and 5, a higher density can be realised by AlN addition (batches 735 and 750). The higher density however, only in some cases resulted in higher modulus and bending strength values.

In the composites, we found the electric behaviors in a wide range from insulator (e.g. pure silicon nitride) towards conductor state depending on type and the amount of carbon content. The insulator–conductor transition, where the

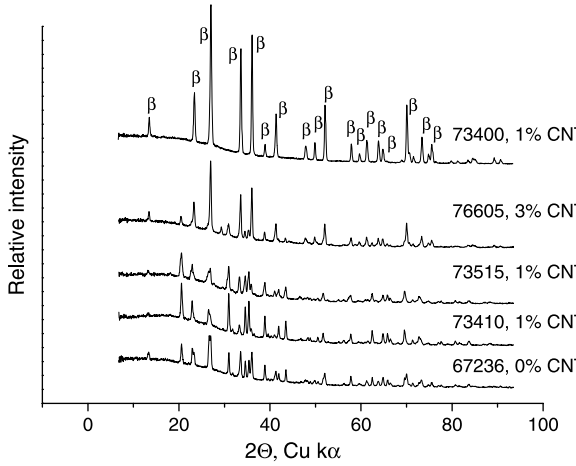

Fig. 3. X-ray diffractograms of sintered samples. The main lines of α-Si_3N_4 and β-Si_3N_4 can be recognized in the case of all samples. The β-Si_3N_4 lines are marked on the 73400 (1% CNT) sample.

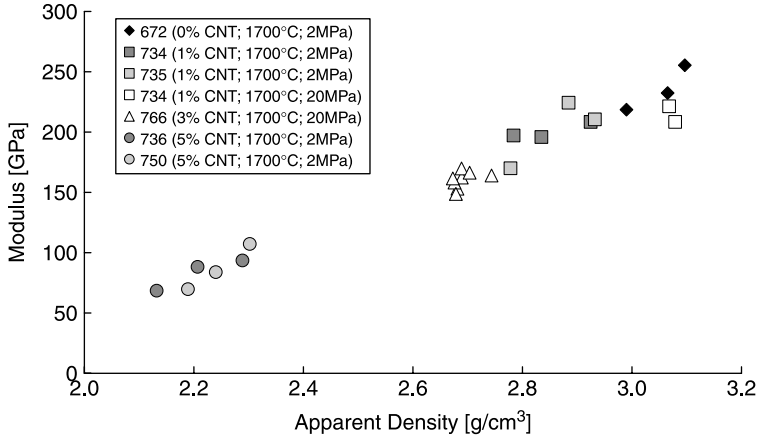

Fig. 4. Modulus of elasticity of reference samples and composites in function of apparent density.

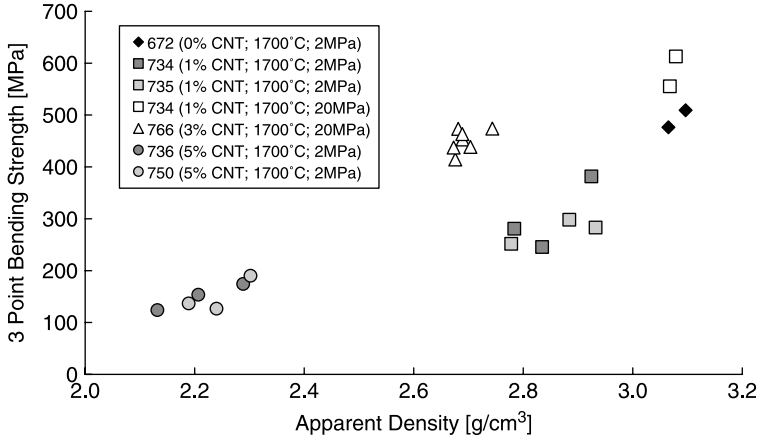

Fig. 5. Three point bending strength of reference samples and composites in function of apparent density.

conductivity changes by many orders, is concentrating in a narrow additive concentration range depending on additives shape, size distribution and electric properties [15].

A pronounced conductor character have been found in the case of samples displayed in Table 2. It is worth to mention that these samples showed the same DC conductivity values in AC measurements or other words the AC conductivity had no frequency dependence up to 100 kHz investigation. From 3 wt% CNT content the composites (these are not shown in Table 2) provided percolation and showed quite similar the same conductivity than in the case of 5 wt% CNT series.

The other branch of samples remained insulator in spite of conducting additives (e.g. 0 wt% CNT-base material, 1 wt% CNT, 1 wt% CB, 1 and 5 wt% Graphite), the conductor particles could not develop percolation tracks for current paths. The AC impedance plots of high DC resistance samples are displayed in Fig. 6. It shows the imaginary parts of complex impedance versus real parts. The imaginary part, which represents the capacitive character is more dominant over the frequency range, means that the samples work as dielectric insulator materials between contact surfaces, forming a capacitor. In Fig. 7, the absolute impedance versus frequency is displayed. Except 5 wt% graphite sample all the curves run with −1 slop in a log–log plot means that the impedance has $1/\omega$ dependence on frequency. This is a typical capacitive impedance feature ($R_c = -i/C\omega$). The insulator samples changed their high DC impedance due to frequency variation of capacitive impedance (R_c) which is characteristic to dielectric materials. These dielectric properties do not change in the frequency range. Resistive losses exists from the point of view of dielectric approach which need further dielectric investigations.

As it can be observed in Fig. 7, the 5 wt% graphite sample presents an exception related to insulator character. Presumably this concentration is close to the percolation threshold

Table 2
DC conductivity of conductor type composites

Additives of Si_3N_4 sample	Specific conductivity (S/m)	Sample number	Batch
5% CNT	4.32	73606	736
5% CNT	5.58	73603	
5% CNT	12	73625	
5% CNT	6.9	73635	
5% CNT	7.19	73600	
5% CNT	9.36	75006	750
5% CNT	130	75030	
5% CB	884	75103	751
10% CB	1657	72833	728
10% Graphite	0.82	73031	730

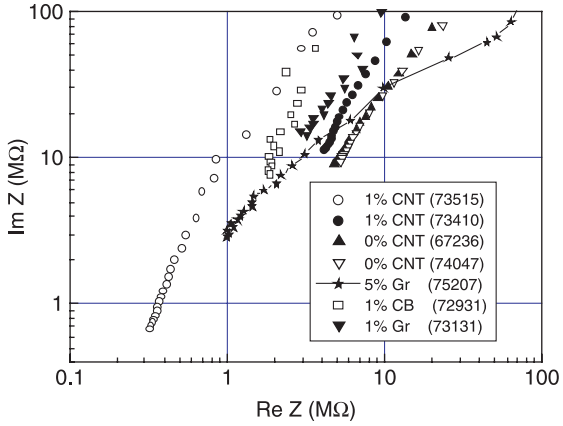

Fig. 6. Impedance plot of different carbon added Si_3N_4 ceramics up to 100 kHz frequency.

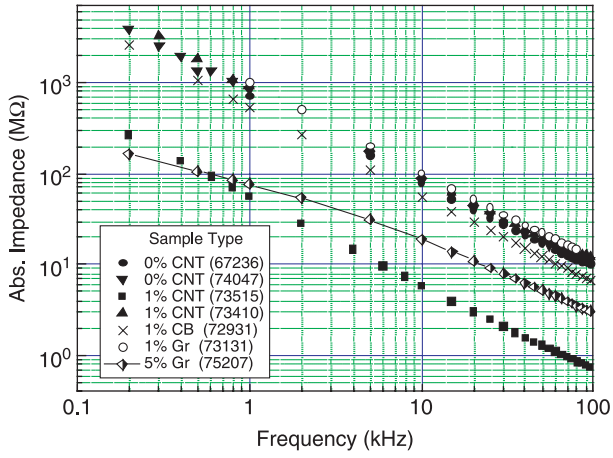

Fig. 7. Absolute impedance versus frequency of different carbon added Si_3N_4 ceramics.

since the frequency dependence getting weaker in the small frequency ranges. It seems that the same carbon type and content samples show scattering electric properties which may related to the altering compositional and structural features, porosity difference and other technological details of sintering processes.

4. Conclusions

Optimisation of the manufacturing processes has been performed in order to thoroughly disperse the carbon nanotube in matrix, to assure a good nanotube-silicon nitride contact and to keep intact the nanotubes during high temperature processing. With increasing the carbon nanotube content a decrease of modulus and strength have been observed. The decrease of modulus and strength can be related to the lower densification rate. Higher density, similar modulus and higher strengths were achieved by increasing the pressure and holding time. With AlN addition more densified samples could be realised, however mechanical improvements have not been observed. As a conductive phase, the AlN addition had a positive effect to specific conductivity. The carbon addition may drastically change the electric properties of composites. Depending on the carbon addition type and concentration (0–5 wt% CNT or 0–10 wt% graphite or 0–10 wt% black carbon) we can yield insulator and low resistance conductor. The measured DC conductivity of low resistance samples proved to be constant up to 100 kHz. The impedance of the good insulator samples became measurable only at higher frequencies. These samples showed typical capacitive feature, worked as constant parameter dielectric material between contact plates. The carbon additives mainly govern the electrical properties, such as insulator–conductor transition, but other parameters as porosity and morphology strongly modify the actual parameters at a given carbon additive type.

The same AC measurements in an extended frequency range and dielectric investigation can give more information to the electrical properties of silicon nitride ceramics with carbon additions.

Acknowledgements

This work was supported by OTKA Foundation (Nos T 043704 and T 043685) and EC, contract NANOCOMP, HPRT-CT-2000-00037 and, EC5 Center of Excellence ICAI-CT-2000-70029.

Dr Csaba Balázsi thanks for OTKA Postdoctoral Research Grant (D38478) and János Bolyai Research Grant. Dr Zoltán Kónya acknowledges the support of the Magyary Zoltán Postdoctoral Fellowship.

References

[1] Rochie S. Carbon nanotubes: exceptional mechanical and electrical properties. Ann Chim Sci Mater 2000;25:529–32.
[2] Thostenson ET, Ren Z, Chou TW. Advances in the science and technology of carbon nanotubes and their composites: a review. Compos Sci Technol 2001;61:1899–912.
[3] Lau KT, Hui D. The revolutionary creation of new advanced materials—carbon nanotube composites. Composites Part B 2002;33:263–77.
[4] Lau KT, Hui D. Effectiveness of using carbon nanotubes as nano-reinforcements for advanced composite structures. Carbon 2002;40:1597–617.
[5] Dong SR, Tu JP, Zhang XB. An investigation of the sliding wear behavior of Cu-matrix composite reinforced by carbon nanotubes. Mater Sci Eng A 2001;313:83.
[6] Ma RZ, Wu J, Wei BQ, Liang J, Wu DH. Processing and properties of carbon nanotubes-nano-SiC ceramic. J Mater Sci 1998;33:5243–63.
[7] Balázsi Cs, Kónya Z, Wéber F, Biró LP, Arató P. Preparation and characterization of carbon nanotube reinforced silicon nitride composites. Mater Sci Eng C 2003;23/6-8:1133–7.
[8] Zhan G-D, Kuntz JD, Wan J, Mukherjee AK. Single-wall carbon nanotubes as attractive toughening agents in alumina-based nanocomposites. Nat Mater 2003;2:38–42.
[9] Zhan G-D, Kuntz JD, Garay JE, Mukherjee AK. Electrical properties of nanoceramics reinforced with ropes of single-walled carbon nanotubes. Appl Phys Lett 2003;83(6).
[10] Curtin WA, Sheldon BW. CNT-reinforced ceramics and metals. Mater Today 2004;7(11):44–9.
[11] Wang X, Padture NP, Tanaka H. Contact-damage-resistant ceramic/single-wall carbon nanotubes and ceramic/graphite composites. Nat Mater 2004;3:539–44.

[12] Kuntz JD, Zhan G-D, Mukherjee AK. Nanocrystalline-matrix ceramic composites for improved fracture toughness. MRS Bull 2004;29(1): 22–7.
[13] Kónya Z, Vesselényi I, Niesz K, Kukovecz A, Demortier A, Fonseca A, et al. Large scale production of short functionalized carbon nanotubes. Chem Phys Lett 2002;360:429–35.
[14] Heitjans P, Indris S. Diffusion and ionic conduction in nanocrystalline ceramics. J Phys Condens Matter 2003;15:1257–89.
[15] McLachlan DS, Blaszkiewicz MB, Newman RE. Electrical resistivity of composites. J Am Ceram Soc 1990;73(8):2187–203.
[16] Balázsi Cs, Kónya Z, Kasztovszky Zs, Wéber F, Vértesy Z, Biró LP, et al. Examination of the carbon nanotube reinforced silicon nitride composites. Proceedings of the fifth international conference on high temperature ceramic matrix composites (HTCMC-5), New Frontiers and Horizons, Seattle, Washington, DC: American Ceramic Society; 2004. p. 107–12.